Invited Paper

Controlling fluorescent proteins by manipulating the local density of photonic states

Christian Blum[a], Yanina Cesa[a], Johanna M. van den Broek[b], Allard P. Mosk[b], Willem L. Vos[b,c], and Vinod Subramaniam[a]

[a] Biophysical Engineering Group, Faculty of Science and Technology and MESA+ Institute for Nanotechnology, University of Twente, P.O. Box 217, 7500 AE Enschede, The Netherlands.
[b] Complex Photonic Systems (COPS), Faculty of Science and Technology and MESA+ Institute for Nanotechnology, University of Twente, P.O. Box 217, 7500 AE Enschede, The Netherlands.
[c] Photonic Bandgaps Group, Center for Nanophotonics, FOM Institute AMOLF, Kruislaan 407, 1098 SJ Amsterdam, The Netherlands
c.blum@tnw.utwente.nl

ABSTRACT

We present the first demonstration of control of the emission lifetime of a biological emitter by manipulating the local density of optical states (LDOS). LDOS control is achieved by positioning the emitters at defined distances from a metallic mirror. This results in a characteristic oscillation in the fluorescence decay rate. Since only the emitting species contribute to the emission lifetimes, the radiative and nonradiative decay rates derived from the lifetime changes characterize specifically the on- states of the emitter. We have thus experimentally determined the decay rates, and by extension the quantum efficiency and emission oscillator strength, of exclusively the emitting states of the widely used Enhanced Green Fluorescent Protein (EGFP). This approach is in contrast to other methods that average over emitting and dark states. The quantum efficiency of the on-states determined for EGFP is 72%. This value is higher than previously reported values determined by methods that average over on- and off-states, as is expected for this system with known dark states. The method presented is especially interesting for photophysically complex systems like fluorescent proteins, where a range of emitting and dark forms has been observed.

Keywords: Fluorescent Proteins, GFP, Photophysics, Quantum efficiency, LDOS, fluorescence lifetime,

1. INTRODUCTION

The visualization of molecular and cellular biological processes by fluorescence microscopy has been revolutionized by the discovery, development, and use of genetically–encodable visible fluorescent proteins (VFPs) [1-3]. Due to the widespread use of VFPs as reporters and sensors, a deep understanding of the versatile photophysics of fluorescent proteins is essential and is the focus of intense research [4-8]. It has been shown that different chromophores can form within one protein [6, 9], intrinsic and photoinduced spectral shifts have been observed [10-12], and it has been demonstrated that VFPs exhibit blinking on different timescales as a result of transitions between emitting and non-emitting states [13-15].

The coexistence of fluorescent protein subensembles within one sample influences the determination of fundamental emission properties such as the radiative and nonradiative decay rates, fluorescence quantum efficiency, and oscillator strength, since most approaches average over the different subensembles. The most widely-used method to determine the quantum efficiency of an unknown fluorophore is to compare the wavelength integrated emission intensity of the unknown sample to a known reference having the same absorbance at the chosen excitation wavelength [16]. From the determined quantum efficiency and the measured fluorescence lifetime, the radiative and non-radiative decay rates, and

Advanced Microscopy Techniques, edited by Paul J. Campagnola, Ernst H. K. Stelzer, Gert von Bally, Proc. of SPIE-OSA Biomedical Optics, SPIE Vol. 7367, 73670C · © 2009 SPIE-OSA · CCC code: 1605-7422/09/$18 · doi: 10.1117/12.831551

by extension the emission oscillator strengths, can be calculated. However, this approach is rigorously correct only for ensembles of identical emitters. The method does not discriminate between molecules in (a) emitting states and in (b) absorbing but non-emitting states or (c) in photoinduced dark states created by the measurement itself. Clearly the averaging over the dark states biases the determined quantum efficiency towards smaller values and hence affects the calculated values for the decay rates and oscillator strength.

Especially for photophysically complex systems like fluorescent proteins, the published values for photophysical parameters can vary significantly. A typical example is the reported quantum efficiency of the red emitting protein DsRed, for which the values in the literature range from 23% [17] to the much higher current consensus values, but which nonetheless range from 68% [18, 19] to 79% [20]. Another example is the green emitting protein Azami green, for which quantum efficiencies of 67% [21] and 90% [22] were reported.

To gain insight into the photophysics of complex systems, a method to determine quantum efficiencies that is independent of the presence of non-emitting states and does not rely on relative measurements would be of great value. We recently presented a method to determine the radiative and nonradiative decay rates of exclusively the emitting states of an emitter [23]. The method is based on positioning the emitters at precisely defined distances from a metallic mirror and thereby controlling the local density of optical states. From a classical point of view, if an emitter is placed in front of a metallic mirror, the field emitted directly by the emitter interferes with the field reflected by the mirror. Depending on the distance from the mirror we can observe constructive or destructive interference. If the interference is constructive, the local density of states, and hence the emission rate, will be increased. If on the other hand, the interference is destructive, the local density of states, and hence the emission rate, will be reduced (see schematic in Fig 2a)). In this way we control the local density of states by controlling the distance from the emitters to the mirror. A classical model taking full account of material properties of the mirror and dielectric environment was developed by Chance et al [24].

The distance-dependent modification of the local density of states results in a characteristic oscillation in the fluorescence decay rate [24-27] that we monitored by fluorescence lifetime microscopy. Analyzing the change of emission lifetime as a function of the emitter distance to the mirror gives access to the decay rates, quantum efficiency and emission oscillator strength. Since only emitting states contribute to the emission lifetime, only the properties of the emitting states are determined, in contrast to other methods that average over emitting and non-emitting states.

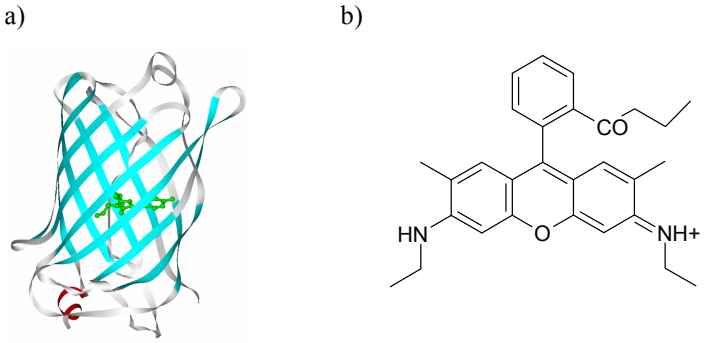

Fig. 1 (a) Structure of the green fluorescent protein EGFP. EGFP is a typical representative of the class of genetically-encodable fluorescent proteins. The emitting chromophore is completely shielded by the protein scaffold from the external environment and forms in an autocatalytic process inside of the protein. Fluorescent proteins show very complex photophysics, e.g. different dark states have been demonstrated, which greatly complicate the determination of photophysical parameters by conventional methods. (b) Structure of Rhodamine 6G. Rhodamine 6G is a common and well-characterized laser dye with relatively simple photophysics that we used to validate our method.

The control of the local density of states to modify the emission lifetime has been applied in other research fields to erbium ions [28], semiconductor colloidal nanocrystals [29, 30], silicon nanocrystals [31] and self-assembled quantum dots [32]. To validate the method for the purpose of determining on-states emission rates and to demonstrate its potential

especially for photophysically complex biological systems we analyzed the widely used visible fluorescent Protein EGFP and Rhodamine 6G. Rhodamine 6G (see Fig 1b)) is a very well characterized and photophysically non complex emitter for which we expect to reproduce with our method the values reported in the literature using conventional methods. EGFP (see Fig 1a)) on the other hand is known for its photophysical complexity, different spectral forms as well as different dark states have been reported in the literature[13-15]. Consequently, we expect to find higher values for the quantum efficiency of the emitting states only than the so-far reported values averaged over emitting and dark states.

2. METHODS

We chose to work in a single mirror configuration to control the local density of states of the emitters. We placed the emitters embedded in an optically isotropic medium at precisely defined distances from a metallic mirror. To realize these conditions we used the sample configuration shown in Fig. 2b).

2.1 Mirror and space layer fabrication

We fabricated the mirrors and spacer layers by multilayer e-gun deposition on a silicon wafer. We first deposited a 50nm chromium adhesion layer that was then covered with the silver layer that acts as the mirror. We deposited optically thick layers of silver of about 200nm. Finally we deposited the SiO_2 layer that acts as spacer between the emitter and the mirror. The thickness of this SiO_2 layer was varied from sample to sample to obtain the selected distance between the emitters and the silver mirror. The whole deposition process was carried out in a Balzers BAK 600 e-gun evaporation machine.

Since the exact determination of the distance between the emitters and the mirror is essential for our analysis, we characterized the mirrors produced by scanning electron microscopy (SEM). We imaged different positions of a cross section of each mirror-spacer. A typical cross section SEM image of the mirror and covering SiO_2 layer is shown in Fig. 2c). For all measured samples the thickness of the silver mirror and of the SiO_2 spacer layer was found to be homogeneous over the analyzed cross sections. Additionally the refractive index of the SiO_2 layer was measured with ellipsometry for the different spacer thicknesses, giving a value of n=1.46±0.05.

2.2 Sample film and cover

On top of the SiO_2 spacer layer we deposited a thin film containing the emitters under study. We chose to embed the emitters (EGFP obtained as reported in [10], Rhodamine 6G from Lambda Physics) into a PVA polymer matrix. Due to the characteristics of the PVA, we easily obtained thin layers by spincasting the polymer-emitters solution onto the SiO2 spacers, and a nearly isotropic orientation of the molecules on the layer. We used a solution of PVA (1% PVA per weight in water) and the corresponding molecule at low concentrations to exclude dye-dye interactions.

Samples of 2 cm x 2 cm were cut from the original wafer and 100 μl of the PVA solution was spin coated onto each sample at 6000 rpm for 10 seconds. To determine the thickness of the resulting PVA layer we used atomic force microscopy spanning a region containing a scratch made on the layer with a Teflon tweezers, finding an homogeneous layer of 17±3 nm. As a result, the total distance between the emitters and the mirrors is defined by the spacer thickness plus half the PVA layer thickness, which is held constant for all samples.

To achieve optically isotropic embedding of the emitters essential for the single mirror configuration used [24], we deposited a thick layer of PMMA (n = 1.489) onto the fluorescent layer matching the refractive index of the spacer. A drop of ~2% PMMA in toluene solution was deposited and dried over the sample to form a layer > 1 μm.

To determine the lifetime of the emitters in a homogeneous medium with the refractive index of the spacer, we used as substrate a quartz coverslip which has a refractive index of n = 1.46, and followed the same sample film and cover production procedure.

2.3 Emission Lifetime determination

The fluorescence decay curves were measured using a time correlated single photon counting (TCSPC) system (for details see [33]). The emitters were excited by a pulsed diode laser with a wavelength of 469 nm, pulse duration of 50 ps

(FWHM) and a repetition rate of 20MHz (BDL475, 469nm, B&H, Germany). We worked in an epi-illumination configuration using the same objective (40x, NA 0.6) for illumination and collection of emitted photons. A 10 nm band pass emission filter centered at 510 nm was used for EGFP, and a 15 nm band pass emission filter centered at 556 nm was used for Rhodamine 6G to limit the detection wavelength to the peak of the emission spectrum of the respective emitters. To eliminate any influence by scattered or back-reflected excitation light, an additional long pass filter (razor edge 473.0 nm, Semrock, USA) was inserted into the detection path. The emission was focused to the active area of a single photon avalanche diode (PDM series, MPD, Italy, peak quantum efficiency of ~50% at 500 nm) connected to the TCSPC module (SPC-830, Becker & Hickl, Germany) to perform time resolved fluorescence measurements. We chose integration times per decay curve to yield a total of approximately 20000 counts per decay curve to assure accurate determination of the characteristic lifetime (τ) [34] by the TCSPC card software (SPCimage, B&H, Germany).

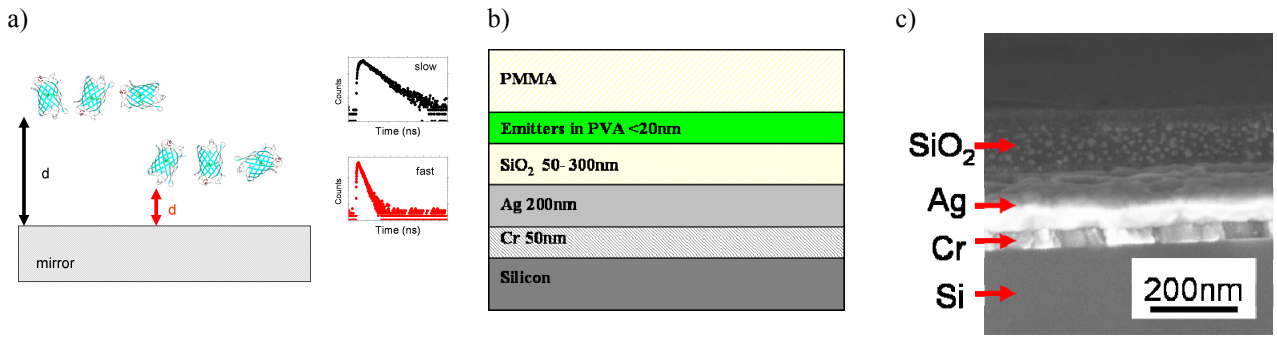

Fig. 2. a) A metallic mirror in the vicinity of an emitter modulates the local density of photonic states, resulting in a change in emission lifetime. b) Schematic of the sample design used to modulate the local density of states. A thin Cr layer deposited on a silicon substrate improves the adherence of the silver layer that acts as a mirror. A SiO_2 layer of well-defined thickness in the range 50 nm to 300 nm is deposited on the mirror and acts as a spacer. The thin <20 nm PVA layer containing the emitters is spincoated on top of the spacer. Finally a thick layer of PMMA of matching refractive index to SiO_2 is used to create an optically isotropic environmet.(c) A typical cross section SEM image of the mirror and covering SiO_2 layer. We imaged and measured different positions of a cross section of each mirror-spacer, finding homogeneous layer thickness for all the samples.

3. RESULTS AND DISCUSION

We determined the characteristic EGFP decay times for six precisely defined sample-mirror distances ranging from 60 nm to 260 nm plus one reference sample with nominally infinite distance from the sample to the mirror.

A typical fluorescence decay curve for EGFP on a mirror with 150 nm emitter-mirror distance is presented in Figure 3 a). All data obtained was fitted by a monoexponential decay function to obtain the characteristic decay time. The quality of the fit was judged by the χ^2 parameter, where a $\chi^2 = 1$ is characteristic of an accurate fit. The residuals plotted at the bottom of the figure show that the fitting is good in the whole range of the decay.

For the method used, the very accurate determination of the characteristic decay time for each precisely defined sample-mirror distance is essential. However, small variations in the thickness of the spacer and sample-containing layers defining the distance to the mirror, as well as variations in the fits of the data will give rise to changes in the recorded lifetimes. We therefore decided to use fluorescence lifetime imaging and statistical analysis of a large number of decay curves for each sample, obtaining a lifetime distribution for each sample. For each sample-mirror distance we collected five separate fluorescence lifetime images at different positions, thus accounting for any possible inhomogeneities in the emitter-mirror distance within one sample. Each image covers an area of 16×16 μm^2 and contained 32×32 decay curves, see figure 3b). We assembled the decay times extracted from the monoexponential fitting of the 5120 single pixel decay

curves into one histogram for each sample-mirror distance. From the distribution of lifetimes we can determine the most frequent lifetime as well as the width of the distribution. The width of the distribution of recorded lifetimes is a measure of the quality of the lifetime determination for each dye-mirror distance, and narrow distributions indicate a high quality sample, lifetime recording and analysis.

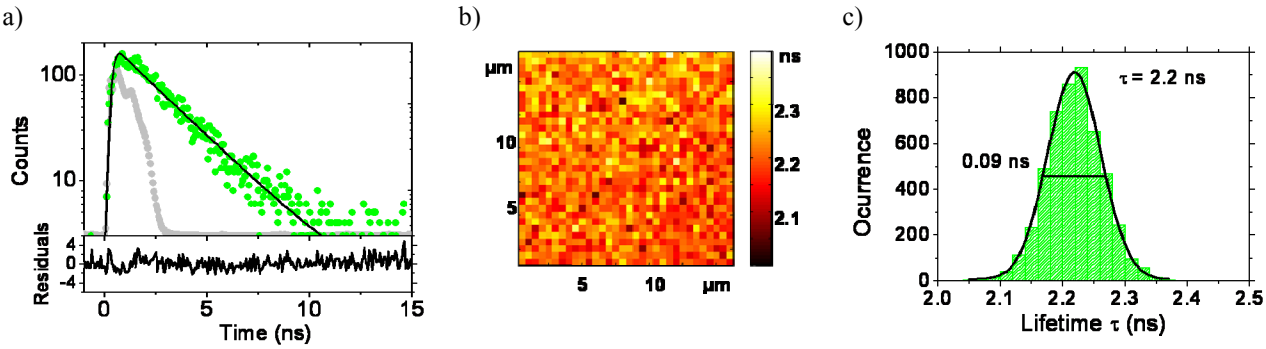

Fig. 3. a) Typical decay curve measured for at a distance of 150 nm to the mirror for EGFP. The data was fitted with a mono exponential decay. The light grey curve corresponds to the instrument response function (IRF) of the system. b) Typical lifetime image, showing the homogeneity of the sample. Each pixel represents the fitted lifetime of a curve like that plotted in a). Several images were taken into account to determine the lifetime distribution for each distance to the mirror. c) Lifetime distribution histogram. The distribution is very narrow and shows a Gaussian shape.

In figure 3c) we show the histogram of lifetimes that results from the detailed analysis above for the EGFP sample-mirror distance of 150 nm. The determined width of the observed lifetime distribution is very narrow (0.09ns), showing the good quality of our sample preparation and measurement. The most frequent lifetime of 2.2 ns is the peak of the Gaussian distribution for a EGFP–mirror distance of 150 nm, resulting in a decay rate of 0.45±0.01 ns^{-1} for the respective distance. For all the samples representing different emitter-mirror distances we find similar Gaussian distributions of lifetimes with FWHM of 0.08±0.01 ns. The peak positions of the most frequent lifetime vary as expected with the emitter-mirror distance, corresponding to the expected modulation of the decay rate.

In the same way we determined the lifetime of a reference sample of EGFP without mirror in a homogeneous medium of refractive index of n = 1.46. The lifetime determined for the reference sample was 2.04 ns, corresponding to a decay rate of 0.49 ns^{-1}. The decay rates normalized with the rate determined for the reference sample plotted as a function of the distance to the mirror are presented in figure 4(a). The error bars on the abscissa are derived from the uncertainties in SiO_2 and PVA layer thicknesses ($\Delta z = \pm 6$ nm), while the error bars for the decay rate were derived using the half-width of the lifetime ($\Delta\tau$ = 0.045 ns). Clearly the decay rates oscillate with increasing distance to the mirror. Further, the oscillation amplitude decreases with increasing distance. Both effects are expected from theory. The measured decay rates follow the values predicted for an isotropic distribution of emitter orientations.

As expected from the moderate quantum efficiency of EGFP, the modulation depth of the decay rate is smaller than that for high quantum efficiency dyes.

The measured total decay rate is the sum of the non-radiative decay rate and the radiative decay rate. According to Fermi's golden rule [35], the radiative decay rate is proportional to the projected local density of optical states (LDOS) and therefore depends explicitly on the distance to the mirror and the transition frequency. On the other hand the non-radiative decay rate is independent of the change of the LDOS and constant in our experiments. In figure 4b) the total decay rate is plotted as a function of the normalized LDOS. The error bars are determined from the uncertainty in the lifetime of half-width of the lifetime distribution ($\Delta\tau$ = 0.045 ns) and from the normalized LDOS, based on the interval corresponding to the sample-mirror distance uncertainty. As expected from Fermi's golden rule a linear relation was found between the measured decay rate and the calculated normalized LDOS. After fitting the data with a linear

function, the non-radiative decay rate can be derived from the offset of the linear function and the radiative decay rate from the slope of the function.

We determine the radiative decay rate to be γ^{hom}_{rad}= 0.36± 0.03ns^{-1} and the nonradiative decay rate to be γ_{nrad}= 0.14γ± 0.03ns^{-1}, resulting a quantum efficiency Q = 72% and an effective emission oscillator strength f_{emiss} = 0.97 [23]. By modulation of the local density of states and observation of the change in emission lifetime, the photophysical properties characteristic of the emitting states of the fluorophore are exclusively addressed, because non-emitting states do not contribute to the observed emission lifetime and are thus not accounted for. Conventional measurements are adversely affected by absorbing and non-emitting as well as non-absorbing states photoinduced during the measurement process, so that we expected to find an increased value for the on state quantum efficiency in our measurement. Indeed the value for the quantum efficiency we obtain (72%) is markedly higher than the value of Q=60% reported before [19]. This is consistent with reports that a significant fraction of green emitting proteins can reside in dark states even at very low excitation intensities [36].

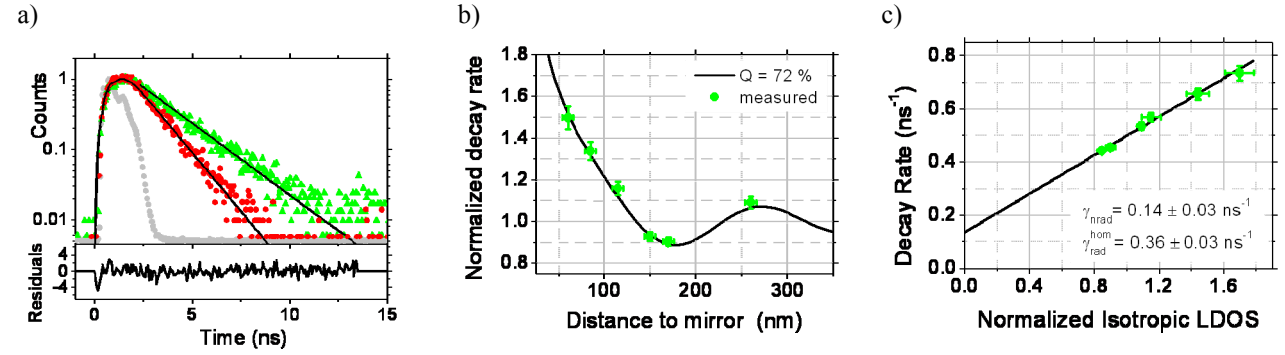

Fig. 4. a) Typical decay curve measured for EGFP for distances to the mirror of 60nm (circles) and 170nm (triangles). At shorter distances to the mirror a shorter lifetime is observed (τ = 2.26 ns, χ^2 = 1.02 for 170 nm and τ = 1.36 ns, χ^2 = 1.6 for 60 nm), as predicted by the theory. b) Normalized decay rate vs the distance to the interface for EGFP. The measured values (circles) follow the predicted behavior for Q = 72% and isotropic dipole orientation (solid line), c) Total decay rate as a function of the normalized LDOS. The linear fit (solid line) yields values of the nonradiative decay and the radiative decay rate; from these decay rates the quantum efficiency is calculated to be 72% ± 6%.

To validate our approach we determined the quantum efficiency of the photophysically well-defined and characterized dye Rhodamine 6G. Although dark states have been observed for Rhodamine 6G, all these dark states have been found to be linked to the triplet state [37]. The probability for inter-system crossing to the triplet state for Rhodamine 6G is generally low enough to exclude a noticeable buildup of molecules in the triplet state, under the conditions applied. Thus we did not expect a difference in the determined quantum efficiency using our method compared to conventional methods. We determine the quantum efficiency of Rhodamine 6G to be 95%+-5%. This value agrees excellently with the values reported in the literature, where values ranging from 0.94 to 0.96 [38-42] can be found.

4. CONCLUSIONS

We have presented a method to determine the radiative and non radiative decay rates of exclusively the emitting states of a fluorescent protein. We systematically changed the local density of optical states by positioning the fluorescent protein at precisely defined distances from a metallic mirror, which results in characteristic modulation of the emission lifetime. Analyzing the oscillation of emission lifetime as a function of the emitter-mirror distance gives access to the decay rates, quantum efficiency and emission oscillator strength. Since only emitting states contribute to the emission lifetime, only the properties of the emitting states are determined. Also no reference molecule is needed. This makes the determination of the decay rates by changing the local density of optical states an especially potent method to analyze complex

photophysical systems like fluorescent proteins, a class of molecules which are known to exhibit significant residence times in intrinsic or photoinduced dark states. We even envision the individual characterization of different emitting forms coexisting in many fluorescent proteins. In this case, the decay characteristics are multiexponential, and the influence of a modified local density of photonic states on each individual decay component can be analyzed. To modulate the local density of optical states to a greater extent than what can be achieved using mirrors, the emitter can be infiltrated into photonic crystals. We have recently shown that fluorescent proteins stay fluorescent when inside a photonic crystal and that the apparent emission color can be photonically tuned [43].

Acknowledgements

We thank Niels Zijlstra and Merel Leistikow for their contribution to the LDOS calculations and Willem Tjerkstra for useful discussions. This work is part of the research program of the "Stichting voor Fundamenteel Onderzoek der Materie" (FOM), which is supported by the "Nederlandse Organisatie voor Wetenschappelijk Onderzoek" (NWO). W.L.V. also thanks NWO-Vici and STW/NanoNed. C.B., Y.C. and V.S. also acknowledge support from the MESA$^+$ Institute for Nanotechnology.

REFERENCES

[1] Chalfie, M., Y. Tu, G. Euskirchen, W. W. Ward, and D. C. Prasher, "Green Fluorescent Protein As A Marker For Gene-Expression," Science, 263(5148), 802-805 (1994).

[2] Lippincott-Schwartz, J., and G. H. Patterson, "Development and use of fluorescent protein markers in living cells," Science, 300(5616), 87-91 (2003).

[3] Yu, J., J. Xiao, X. J. Ren, K. Q. Lao, and X. S. Xie, "Probing gene expression in live cells, one protein molecule at a time," Science, 311(5767), 1600-1603 (2006).

[4] Creemers, T., A. Lock, V. Subramaniam, T. Jovin, and S. Völker, "Photophysics and optical switching in green fluorescent protein mutants," Proc. Natl. Acad. Sci. U. S. A. , 97(7), 2974-2978 (2000).

[5] Jung, G., J. Wiehler, and A. Zumbusch, "The photophysics of green fluorescent protein: influence of the key amino acids at positions 65, 203, and 222," Biophys. J. , 88(3), 1932-47 (2005).

[6] Remington, S. J., "Fluorescent proteins: maturation, photochemistry and photophysics," Current Opinion in Structural Biology, 16(6), 714-721 (2006).

[7] Schleifenbaum, F., C. Blum, K. Elgass, V. Subramaniam, and A. J. Meixner, "New insights into the photophysics of DsRed by multiparameter spectroscopy on single proteins," Journal of Physical Chemistry B, 112(25), 7669-7674 (2008).

[8] Blum, C., and V. Subramaniam, "Single-molecule spectroscopy of fluorescent proteins," Analytical and Bioanalytical Chemistry, 393(2), 527-541 (2009).

[9] Verkhusha, V. V., D. M. Chudakov, N. G. Gurskaya, S. Lukyanov, and K. A. Lukyanov, "Common pathway for the red chromophore formation in fluorescent proteins and chromoproteins," Chemistry & Biology, 11(6), 845-854 (2004).

[10] Blum, C., A. J. Meixner, and V. Subramaniam, "Room temperature spectrally resolved single-molecule spectroscopy reveals new spectral forms and photophysical versatility of Aequorea green fluorescent protein variants," Biophysical Journal, 87(6), 4172-4179 (2004).

[11] Blum, C., A. J. Meixner, and V. Subramaniam, "Spectral Versatility of Single Reef Coral Fluorescent Proteins Detected by Spectrally-Resolved Single Molecule Spectroscopy," ChemPhysChem, 9(2), 310-315 (2008).

[12] Malvezzi-Campeggi, F., M. Jahnz, K. G. Heinze, P. Dittrich, and P. Schwille, "Light-induced flickering of DsRed provides evidence for distinct and interconvertible fluorescent states," Biophysical Journal, 81(3), 1776-1785 (2001).
[13] Hendrix, J., C. Flors, P. Dedecker, J. Hofkens, and Y. Engelborghs, "Dark states in monomeric red fluorescent proteins studied by fluorescence correlation and single molecule spectroscopy," Biophysical Journal, 94(10), 4103-4113 (2008).
[14] Garcia-Parajo, M. F., J. A. Veerman, R. Bouwhuis, R. Vallee, and N. F. van Hulst, "Optical probing of single fluorescent molecules and proteins," Chemphyschem, 2(6), 347-360 (2001).
[15] McAnaney, T. B., W. Zeng, C. F. E. Doe, N. Bhanji, S. Wakelin, D. S. Pearson, P. Abbyad, X. H. Shi, S. G. Boxer, and C. R. Bagshaw, "Protonation, photobleaching, and photoactivation of yellow fluorescent protein (YFP 10C): A unifying mechanism," Biochemistry, 44(14), 5510-5524 (2005).
[16] Lakowicz, J., [Principles of Fluorescence Spectroscopy] Kluwer Academic / Plenum Publishers, New York(1999).
[17] Matz, M. V., A. F. Fradkov, Y. A. Labas, A. P. Savitsky, A. G. Zaraisky, M. L. Markelov, and S. A. Lukyanov, "Fluorescent proteins from nonbioluminescent Anthozoa species," Nature Biotechnology, 17(10), 969-973 (1999).
[18] Bevis, B. J., and B. S. Glick, "Rapidly maturing variants of the Discosoma red fluorescent protein (DsRed)," Nature Biotechnology, 20(1), 83-87 (2002).
[19] Patterson, G., R. N. Day, and D. Piston, "Fluorescent protein spectra," Journal of Cell Science, 114(5), 837-838 (2001).
[20] Campbell, R. E., O. Tour, A. E. Palmer, P. A. Steinbach, G. S. Baird, D. A. Zacharias, and R. Y. Tsien, "A monomeric red fluorescent protein," Proc Natl Acad Sci U S A, 99(12), 7877-82 (2002).
[21] Karasawa, S., T. Araki, M. Yamamoto-Hino, and A. Miyawaki, "A Green-emitting fluorescent protein from Galaxeidae coral and its monomeric version for use in fluorescent labeling," Journal of Biological Chemistry, 278(36), 34167-34171 (2003).
[22] Dai, M. H., H. E. Fisher, J. Temirov, C. Kiss, M. E. Phipps, P. Pavlik, J. H. Werner, and A. R. M. Bradbury, "The creation of a novel fluorescent protein by guided consensus engineering," Protein Engineering Design & Selection, 20(2), 69-79 (2007).
[23] Cesa, Y., C. Blum, J. M. van den Broek, A. P. Mosk, W. L. Vos, and V. Subramaniam, "Manipulation of the local density of photonic states to elucidate fluorescent protein emission rates," Physical Chemistry Chemical Physics, 11(14), 2525-2531 (2009).
[24] R.R.Chance, A.Prock, and R.Silbey, [Advances in chemical physics] Wiley & Sons, New York(1978).
[25] Amos, R. M., and W. L. Barnes, "Modification of the spontaneous emission rate of Eu3+ ions close to a thin metal mirror," Physical Review B, 55(11), 7249-7254 (1997).
[26] Chance, R. R., A. Prock, and R. Silbey, "Lifetime of an Excited Molecule near a Metal Mirror - Energy-Transfer in Eu3+-Silver System," Journal of Chemical Physics, 60(5), 2184-2185 (1974).
[27] Astilean, S., S. Garrett, P. Andrew, and W. L. Barnes, "Controlling the fluorescence lifetime of dyes in nanostructured geometries," Journal of Molecular Structure, 651, 277-283 (2003).
[28] Snoeks, E., A. Lagendijk, and A. Polman, "MEASURING AND MODIFYING THE SPONTANEOUS EMISSION RATE OF ERBIUM NEAR AN INTERFACE," Physical Review Letters, 74(13), 2459-2462 (1995).
[29] Brokmann, X., L. Coolen, M. Dahan, and J. P. Hermier, "Measurement of the radiative and nonradiative decay rates of single CdSe nanocrystals through a controlled modification of their spontaneous emission," Physical Review Letters, 93(10), 107403 (2004).
[30] Leistikow, M. D., J. Johansen, A. J. Kettelarij, P. Lodahl, and W. L. Vos, "Size-dependent oscillator strength and quantum efficiency of CdSe quantum dots controlled via the local density of states," Physical Review B (Condensed Matter and Materials Physics), 79(4), 045301 (2009).
[31] Walters, R. J., J. Kalkman, A. Polman, H. A. Atwater, and M. J. A. de Dood, "Photoluminescence quantum efficiency of dense silicon nanocrystal ensembles in SiO2," Physical Review B, 73(13), 132302 (2006).
[32] Johansen, J., S. Stobbe, I. S. Nikolaev, T. Lund-Hansen, P. T. Kristensen, J. M. Hvam, W. L. Vos, and P. Lodahl, "Size dependence of the wavefunction of self-assembled InAs quantum dots from time-resolved optical measurements," Physical Review B, 77(7), 073303 (2008).
[33] Blum, C., Y. Cesa, M. Escalante, and V. Subramaniam, "Multimode microscopy: spectral and lifetime imaging," Journal of the Royal Society Interface, 6, S35-S43 (2009).

[34] Maus, M., M. Cotlet, J. Hofkens, T. Gensch, F. C. De Schryver, J. Schaffer, and C. A. M. Seidel, "An experimental comparison of the maximum likelihood estimation and nonlinear least squares fluorescence lifetime analysis of single molecules," Analytical Chemistry, 73(9), 2078-2086 (2001).
[35] Loudon, R., [The quantum theory of light] Oxford University Press, Oxford ; New York(2000).
[36] Jung, G., S. Mais, A. Zumbusch, and C. Brauchle, "The role of dark states in the photodynamics of the green fluorescent protein examined with two-color fluorescence excitation spectroscopy," Journal of Physical Chemistry A, 104(5), 873-877 (2000).
[37] Zondervan, R., F. Kulzer, S. B. Orlinskii, and M. Orrit, "Photoblinking of rhodamine 6G in poly(vinyl alcohol): Radical dark state formed through the triplet," Journal of Physical Chemistry A, 107(35), 6770-6776 (2003).
[38] Drexhage, K. H., [Dye lasers] Springer-Verlag, Berlin ; New York(1973).
[39] Kubin, R. F., and A. N. Fletcher, "Fluorescence Quantum Yields of Some Rhodamine Dyes," Journal of Luminescence, 27(4), 455-462 (1982).
[40] Arden, J., G. Deltau, V. Huth, U. Kringel, D. Peros, and K. H. Drexhage, "Fluorescence and Lasing Properties of Rhodamine Dyes," Journal of Luminescence, 48-9, 352-358 (1991).
[41] Fischer, M., and J. Georges, "Fluorescence quantum yield of rhodamine 6G in ethanol as a function of concentration using thermal lens spectrometry," Chemical Physics Letters, 260(1-2), 115-118 (1996).
[42] Delysse, S., J. M. Nunzi, and C. Scala-Valero, "Picosecond optical Kerr ellipsometry determination of S-1 -> S-n absorption spectra of xanthene dyes," Applied Physics B: Lasers and Optics, 66(4), 439-444 (1998).
[43] Blum, C., A. P. Mosk, I. S. Nikolaev, V. Subramaniam, and W. L. Vos, "Color control of natural fluorescent proteins by photonic crystals," Small, 4(4), 492-496 (2008).